J. Biochem. **136**, 509–515 (2004)
DOI: 10.1093/jb/mvh147

The Energetic Conversion Competence of *Escherichia coli* during Aerobic Respiration Studied by ^{31}P NMR Using a Circulating Fermentation System

Yasushi Noguchi[1,*], Yuta Nakai[1], Nobuhisa Shimba[2], Hiroshi Toyosaki[1], Yoshio Kawahara[1], Shinichi Sugimoto[1] and Ei-ichiro Suzuki[2]

[1]Fermentation & Biotechnology Laboratories and [2]Institute of Life Sciences, Ajinomoto Co. Inc., Kawasaki-ku, Kawasaki, 210-8681

Received May 1, 2004; accepted July 24, 2004

To determine the actual potential of the energetic conversion efficiency of *Escherichia coli* during aerobic respiration, apparent P/O ratios (P/O^{app}) under either limited or standard glucose-feeding conditions were estimated. The previously reported circulating fermentation system (CFS) was used, and ^{31}P NMR saturation-transfer (ST) techniques were employed. By coupling with on-line NMR observations, CFS allowed us to evaluate cellular energetics directly, with both the dissolved oxygen tension and glucose feeding precisely controlled to prevent the effect of substrate-level phosphorylation based on aerobic or anaerobic acidogenesis in *E. coli* cells. Phosphate consumption rates under standard and limited glucose-conditions were estimated as 4.62 ± 0.46 and 1.99 ± 0.11 μmol/s g of dry cell weight (DCW), respectively. Using simultaneously assessed O_2 consumption rates, the P/O^{app} values under these two conditions were estimated as 1.4 ± 0.3 and 1.5 ± 0.1, respectively. To correlate the obtained P/O^{app} values with the potential efficiency of respiratory enzymes, we determined the activities of two NADH dehydrogenases (NDH 1 and 2) and two ubiquinol oxidases (*bo*- and *bd*-type) during the periods when ST was performed. NDH-1 activities in standard or limited glucose cultures were maintained at 57% or 58% of the total NADH oxidizing activity. The percentages of *bo*-type oxidase activity in relation to the total ubiqinol oxidizing activity under the standard and limited glucose conditions were 32% and 36%, respectively. These percentages of enzymatic activities represent the respiratory competence of *E. coli* cells, suggesting that, during the NMR observatory period, the enzymatic activity was not at a maximum, which could also explain the estimated P/O^{app} values. If this is the case, enhancing the expression of the *bo*-type oxidase or disrupting of the *bd*-type oxidase gene could be effective approach to increasing both the P/O ratio and cellular yields.

Key words: energy metabolism, *in vivo* ^{31}P NMR, P/O ratio, saturation transfer.

Abbreviations: DCW, dry cell weight; MDP, methylene diphosphonic acid; P/O^{app}, apparent P/O ratio; DOT, dissolved oxygen tension; CFS, circulating fermentation system; ST, saturation transfer.

An assessment of the energetic competence of the bacterial respiratory chain is of basic and practical importance (*1*). Particularly in aerobic culturing microorganisms, the growth yield depends on both the energy supplies for biomass synthesis and the ATP yield of respiration or respiration efficiency (P/O ratio).

Because *E. coli* cells have several respiratory pathways corresponding to different environmental dissolved oxygen tensions (DOT), they can grow in both aerobic and anaerobic culture (*2*). Under aerobic conditions, the respiratory chain of *E. coli* can function using either of two different membrane-bound NADH dehydrogenases (NDH-1 and NDH-2), and with either of two ubiquinol oxidases (the *bd*- and *bo*-type) (*2*, *3*). The H^+ excretion capacity, which leads to the production of ATP *via* H^+-ATPase, is differs due to the varying combinations of these two sets of enzymes. Further, the expression rates of these two sets of the enzymes change according to the DOT, as the expressions of these enzymes are regulated in an oxygen-dependent manner by the *fnr* and *arc* gene products (*4–6*). Thus, the energetic competence of the enzymes depends on which of the enzymes is utilized for the electron flux (*7*).

A number of studies have been undertaken to examine the influences of respiratory enzymes on cellular energetic efficiency (*8*). However, the direct assessment of the efficiency is particularly difficult because neither ADP nor ATP is taken up by or excreted from intact or growing organisms (*9–11*). To overcome these technical difficulties, ^{31}P NMR saturation-transfer techniques have been introduced to measure directly the rate of ATP turnover in a variety of living systems, including *E. coli*, yeast, and several animal tissues (*12–14*). In such studies, however, little attention has been given to the correlations between oxygen utilization and ATP turnover (*15*). Particularly in NMR experiments, high-density cell cultures

*To whom correspondence should be addressed. Phone: +81 44 210 5898, Fax: +81 44 211 7609, E-mail: yasushi_noguchi@ajinomoto.com

are usually necessary for the quantitative detection of intracellular metabolites resonances. However, these conditions result in low dissolved oxygen tension (DOT) or glucose-mediated aerobic acidogenesis, known as aerobic fermentation (*16*, *17*). Thus, in order to observe the precise energetic production rates derived from oxidative phosphorylation, it is necessary to prevent aerobic or anaerobic fermentation from predominating in energy production that is dependent on excess glucose loading or low DOT tensions (*16*, *17*). To this end, the DOT conditions of the culture should be precisely monitored and controlled.

We have previously constructed a circulating fermentation system (CFS) suitable for *in vivo* NMR observations (*18*, *19*). In this system, the fermentor is composed of a fermentation vessel and two outer tubes through which the medium is circulated by rotary pumps (*18*). These circuits monitor the DOT and metabolites in real-time by an oxygen sensor and an NMR spectrometer, respectively (*18*). Using this device, prolonged NMR spectroscopic measurements, including saturation transfer, can be carried out under various environmental DOTs.

In the present study, we applied saturation-transfer to aerobic respiring *E. coli* of the wild-type strain under two different glucose consumption rates and a controlled DOT conditions, and studied the influences of cellular oxygen consumption on the apparent P/O ratio.

MATERIALS AND METHODS

Bacterial Strain and Culture Conditions—E. coli W3110 were used in this study. The inoculum was prepared in 50 plates of the LB medium, which was composed of 10 g/liter tryptone, 5 g/liter yeast extract, 5 g/liter NaCl, and 20 g/liter bacto-agar. For the *in vivo* NMR experiments, *E. coli* cells were subjected to fermentation in a fermentor, with an initial culture volume of 700 ml kept at 37°C and pH 6.5. Cells were allowed to grow in the medium containing 25 g/liter glucose, 1 g/liter KH_2PO_4, 1 g/liter yeast extract, 0.5 g/liter NaCl, 0.25 g/liter $CaCl_2$, 1 g/liter $MgSO_4.4H_2O$, and 0.05 mg/liter $FeSO_4.7H_2O$. For standard and limited glucose conditions, the glucose concentrations were adjusted to 10 g/liter and 2 g/liter, respectively, by the automatic additions of 10 ml of 500 g/liter glucose solution, respectively.

Measurement of Enzymatic Activities—Ubiquinol oxidase activities were calculated by recording the absorbance changes of ubiquinol-1 at 278 nm with or without 10 μM KCN, as described in the previous study (*20*). The NADH dehydrogenase activities were similarly calculated by measuring the oxidation of NADH and dNADH using the membrane vesicles, as described previously (*21*). All spectrometric measurements were performed at room temperature with a spectrophotometer (Shimadzu MPS-2000).

Fermentation System and DOT Control—For the *in vivo* NMR measurements, the previously constructed circulating fermentation system (CFS) was used (*18*). In this system, the fermentor is composed of a fermentation vessel and two outer tubes through which the medium is circulated by rotary pumps. One tube monitors the dissolved oxygen tension (DOT) via a sensor (tube B), while the other tube monitors metabolites via an NMR spectrometer (tube A). The agitation speed of the fermentor can be automatically regulated to maintain the DOT values in the fermentation vessel at an appropriate level. Additionally, the flow rate and oxygen content of the air blown into the vessel can be altered automatically based on the DOT of the culture medium in Tube B, which is the outer circuit (*18*). We have previously found that DOTs in the fermentation vessel and the two outer tubes installed to measure DOT and NMR can be equilibrated without a significant time-lag (*18*).

The oxygen consumption rates were measured using an exhaust gas analyzer system (Able Co., Tokyo, Japan), and the data were normalized by cell concentration to obtain cellular oxygen consumptions. The temperature of the whole system was kept at 37°C with the aid of a circulating water bath, and acidification was corrected by the automated addition of 10% NH_4OH.

NMR Operation—Using cells at a high density [>5 g of dry cell weight (DCW)/liter], ^{31}P NMR signals were recorded at 160 MHz with a Bruker DSX 400 WB spectrometer, in which 4-k data points were recorded with 1280 transients and a spectral width of 16k Hz. The spectra were typically acquired with the following parameters: pulse width, 34 μs (90° flip angle); repetition time, 1.5 s. To enhance the resolution, the free induction decay was multiplied by an exponential window function prior to Fourier transformation.

Quantification of Intracellular Metabolites—To quantify the culture metabolite content, methylene diphosphonic acid (MDP) in a glass capillary tube in the NMR tube A (see "*Fermentation System and DOT Control*") was used as an internal concentration standard. Here, the ATP and ADP contents were calculated from the ATP-β signal intensities and the ATP-γ signal (including ADP-β signal)–ATP-β signal intensities, respectively. Data obtained were normalized by DCW as described previously (*22*).

Intracellular pH Estimation—To estimate the intracellular pH of *E. coli* cells, a calibration curve for the chemical shift of the inorganic phosphate signal versus pH was obtained experimentally before the *in vivo* NMR observations (data not shown). The intracellular pH values were determined directly from the observed *in vivo* NMR spectra by translating the obtained chemical shift into the calibration curve as described previously (*23*).

Magnetization Transfer—Saturation transfer has generally been used to investigate unidirectional kinetics in equilibrated chemical reaction mixtures (*24*). This technique requires a steady state of the reactant concentrations during measurements (*24*). During our experiments, the concentrations of ATP, ADP, and intracellular inorganic phosphate (P_i^{in}) were maintained at a steady state by using the cells in the stationary phase, and we have observed the effects of saturating the ATP-γ resonance upon the reductions in P_i^{in} signal intensities. The reduction in the intracellular P_i signal intensity when ATP-γ is saturated depends on the apparent rate constants for P_i disappearance (k_F), and k_F is generally obtained from the following equations:

$$k_F = (1/T_{1i} + k_F)(\Delta M_i/M^0_i)$$

Here, the intensity variations are quantitatively described by the modified Bloch equations for spin magnetization in inorganic phosphate (M_i) and ATP-γ phosphate, which exchange via the ATPase reaction (*24*). M^0_i corresponds to the fully relaxed intensities and T_{1i} to the nuclear spin relaxation times in the absence of exchange. The apparent rate constants for P_i consumption (k_F) are obtained by measuring of the steady-state values of ΔM_i and M^0_i, and from an inversion recovery measurement of the apparent T_1 [=1/(1/ T_{1i} + k_F)] performed while the ATP-γ is saturated.

Magnetization transfer experiments, including saturation transfer and inversion recovery, were performed and analyzed following the previously described procedure (*12–14*). A frequency synthesizer driving an auxiliary amplifier that generates the rf field was used to saturate the ATP γ-phosphate resonance in both the estimation of apparent relaxation rates (T_1^{app}) and the ST experiments. In these experiments, spectra from ATP γ-phosphate resonance were compared with those from control irradiation, and the difference was designated as a decrease in the inorganic phosphate peak. In all, 1,280 scans were collected and compared. The T_1^{app} was determined from the slope of the recovery curves obtained from the inversion recovery experiments, which were carried out in the presence of a saturating field at the ATP γ-phosphate by using a 180°–*t*-90° pulse sequence and varying the *t* between 0.5 to 0.6 s. The slopes obtained from these recovery curves provided relaxation times in the presence of exchange. The rates of P_i^{in} consumption were determined by multiplying the change in the fraction of P_i^{in} dependent on the ATP γ-phosphate saturation ($\Delta M = M_o - M$), by the measured apparent T_1 (T_1^{app}) relaxation rate and the intracellular phosphate concentration, as described previously (*12–14*).

Apparent P/O ratio values were calculated from rate of P_i^{in} consumption (flux $P_i \rightarrow$ ATP) and cellular oxygen consumption rates.

Analyses—Optical cell density was measured at 660 nm using a Shimadzu UV260 spectroscopy, and was converted to DCW using the coefficient of k = 2.1, which was obtained using the calibration curve between OD and DCW of *E. coli* cells (data not shown). Glucose concentrations were determined enzymatically using an analyzer (Biotech-Analyzer, Asahi Kasei Co., Tokyo, Japan). The concentrations of acetate in the culture media were assayed by the HPLC (high-performance liquid chromatography) method, as described previously (*25*).

Chemicals—MDP was purchased from Sigma Chemical Co. All other chemicals were commercially available and of the highest grade.

RESULTS AND DISCUSSIONS

Growth Properties of E. coli—To study the influence of cellular oxygen consumption on the apparent P/O ratio, *E. coli* cells were cultured under the following two conditions, as described in Materials and Methods. Under the standard glucose conditions, the feeding rate of the glucose solution was adjusted to maintain a 10 g/liter glucose concentration in the culture medium, so as to maintain the levels of cellular oxygen consumption in the pre-feeding phase (0–6 h). In contrast, the feeding rate under the limited glucose condition was adjusted to maintain a 2 g/liter concentration in the culture medium so as to reduce the cellular oxygen consumption to less than half that in the pre-feeding phase. The typical growth properties of the wild-type *E. coli* strain under these two conditions during the NMR observational period are shown in Fig. 1, a–d. The DOTs were controlled at more than 3% by automatically adjusting the airflow rate and the agitation speed (Fig. 1b). The production of acidic by-products is a major factor in the limitation of high-cell-density

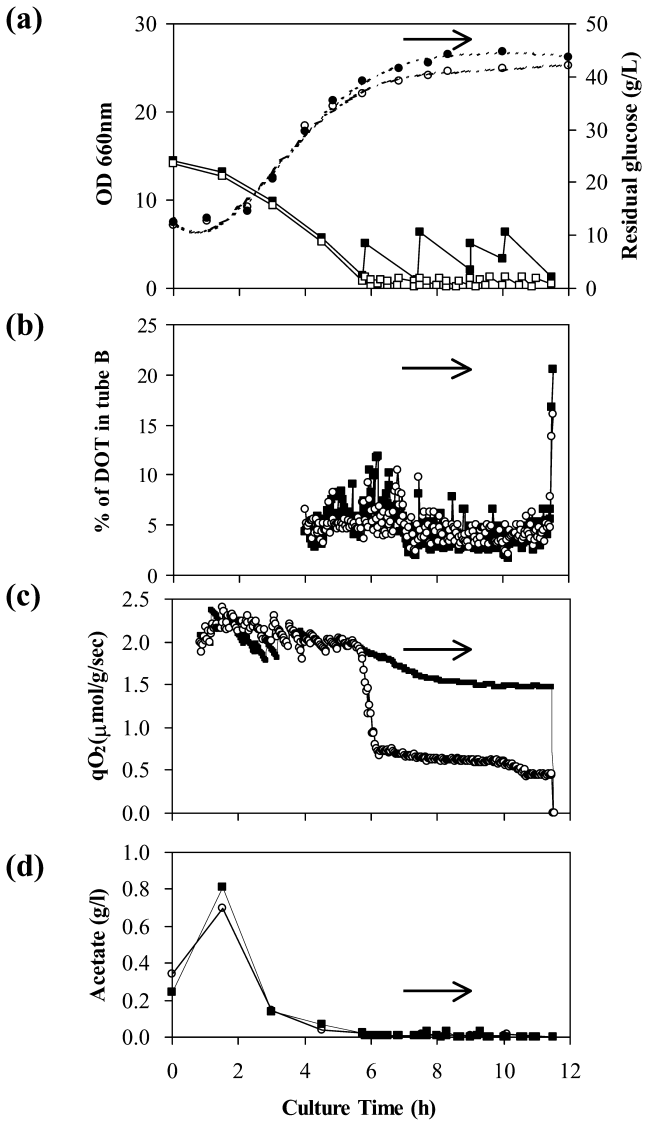

Fig. 1. **Growth properties of the wild type *E. coli* strain during the NMR observation period.** The cells were fed-batch cultured under standard (closed symbols) or limited glucose conditions (open symbols) as described in "MATERIALS AND METHODS." (a) Growth (circles) and residual glucose (squares). (b) DOT values under standard (closed squares) or glucose-limited conditions (open circles). (c) Cellular oxygen consumption under standard (closed squares) or glucose-limited conditions (open circles). (d) Culture acetate accumulation under standard (closed squares) or glucose-limited conditions (open circles). The saturation transfer experiments were performed during the early stationary phase (horizontal bar).

Table 1. **Contents of intracellular metabolites and parameters of *E. coli* cells.**

Conditions (Phase)	Glucose consumption	P_i^{in}	ATP	ADP	ATP/ADP	pH^{in}
	mmol/g of DCW/h	Intracellular content (μmol/g of DCW)				
Standard glucose						
(exponential: 4–6 h)	2.72 ± 0.85	4.8 ± 0.2	3.1 ± 0.1	0.5 ± 0.0	6.5	7.36
(early stationary: 6.5–8.5 h)	1.65 ± 0.18	4.5 ± 0.2	2.7 ± 0.1	0.5 ± 0.0	5.9	7.45
(late satationary: 9–10 h)	1.12 ± 0.07	2.5 ± 0.0	1.3 ± 0.0	0.6 ± 0.0	2.3	7.42
Limited glucose						
(early stationary)	0.75 ± 0.15	4.4 ± 0.1	2.7 ± 0.1	0.5 ± 0.0	5.9	7.45

To quantify the intracellular metabolites, MDP was used as a concentration standard for NMR. Partially relaxed MDP was used to estimate metabolite concentrations. The dry cell weight (DCW) was determined by comparison with an optical density versus dry weight calibration curve. Values are the mean ± SD.

growth, which results from aerobic fermentation (*16*, *17*). Because of this, acetate formation was simultaneously monitored in all experiments as an indicator of aerobic fermentation predominance. In these experiments, DOT tuning and glucose feeding prevented acetate formation during the saturation-transfer experimental phase (arrows) in all trials (Fig. 1d).

In general, the principle of saturation-transfer measurements is to disturb the steady-state equilibrium of the system under investigation and to monitor the response to this perturbation, as described in Materials and Methods. Thus, the saturation-transfer experiments were begun during this stable phase (the early stationary phase; bar in panel a), as the growth rate under both conditions gradually reached a stable value within 6.5 h (Fig. 1a). In these phases, there were significant differences in glucose and oxygen consumption between the two conditions (Fig. 1, a and c, and Table 1).

In Vivo ^{31}P NMR Studies and Estimation of P/O Ratios—Aerobic respiring *E.coli* cells were subjected to *in vivo* ^{31}P NMR observations under a narrowly defined DOT tuning condition. Figure 2, a–d, shows chronological changes in the typical ^{31}P NMR spectra obtained for the standard glucose culture. No signals from extra cellular phosphorylated compounds were detected, except for inorganic phosphate (Fig. 2e).

Concentrations of intracellular metabolites are summarized in Table 1. The parameters of either standard or limited glucose conditions are also incorporated into Table 1. The signal intensities of these parameters should be strictly stabilized in the saturation-transfer experiments. ATP and intracellular inorganic phosphate (P_i^{in}) concentrations under the standard glucose conditions remained almost level until the end of the early stationary phase. After this phase, these values decreased drastically. During the early stationary periods, similar to intracellular inorganic phosphate (P_i^{in}), the ATP and ADP pools remained almost unchanged under the different glucose-loading conditions, and the ATP/ADP ratios did not differ between the two glucose-feeding conditions

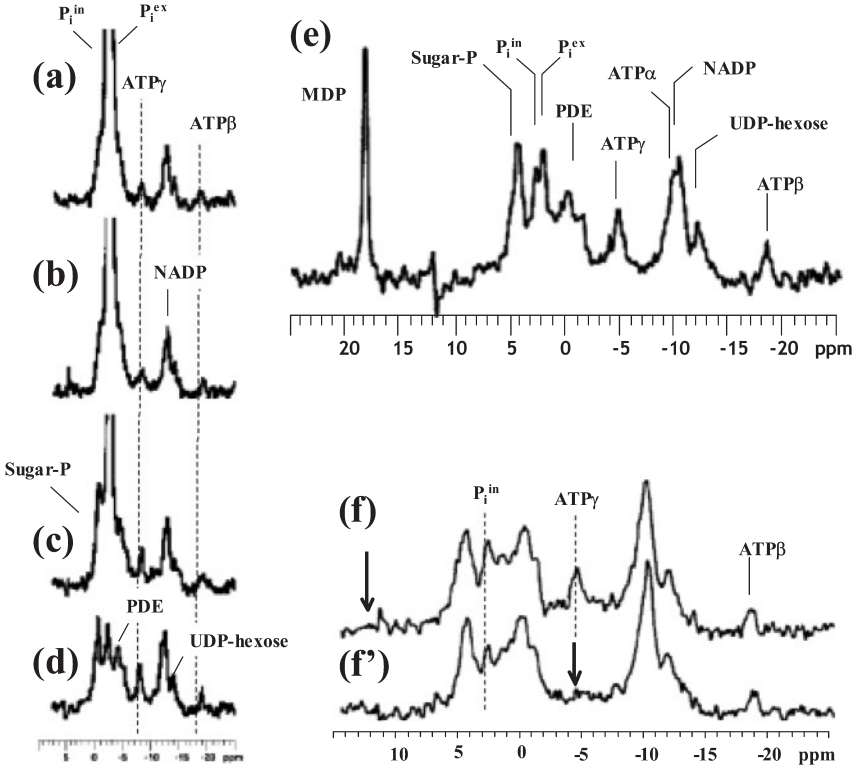

Fig. 2. **Representative 31P NMR spectrum of aerobically respiring *E. coli*.** Spectral changes under standard glucose conditions (a–e). (a) Early exponential phase (2–3 h). (b) Exponential phase (3–4 h). (c) Late exponential (4–6 h). (d) Early stationary (6–7 h). (e) Representative spectrum of the saturation transfer experimental phase. The M^0 (f) and M (f') spectra under standard cultivation conditions were obtained during the early stationary phase by saturation at different positions shown by the arrows. Here, a total of 1,280 scans were collected at the two irradiation frequencies as described in "MATERIALS AND METHODS." Abbreviations for resonances are: methylene diphosphonic acid (MDP), sugar-phosphate (Sugar-P), intracellular inorganic phosphate (Piin), extracellular inorganic phosphate (Piex), phosphodiester (PDE), uridine diphosphate glucose (UDP-glucose), β and γ phosphate of adenine nucleotide phosphates (ATPβ, and ATPγ, respectively). Chemical shifts are given in ppm from 85% H_3PO_4.

Table 2. **Estimation of apparent P/O ratio in aerobic respiring *E. coli* cells.**

Conditions	$\Delta M/M_0$	k_f (s^{-1})	*Flux* ($P_i \rightarrow$ ATP)	O_2 consumption	P/O^{app}
			(μmol/s/g of DCW)		
Standard glucose	0.24 ± 0.14	1.00 ± 0.19	4.62 ± 0.46	1.60 ± 0.10	1.4 ± 0.3
Limited glucose	0.10 ± 0.06	0.45 ± 0.10	1.99 ± 0.11	0.68 ± 0.07	1.5 ± 0.1

Where k_f values were calculated using an apparent relaxation rate T_1^{app} (=0.228+/–0.11) obtained from an inversion recovery experiment as described in "MATERIAL AND METHODS." The dry cell weight (DCW) was determined by comparison with an optical density versus dry weight calibration curve. Values are the mean ± SD.

(Table 1). Intracellular pH values, primarily attributable to chemical shifts in P_i^{in}, did not change during the early stationary phase. Collectively, as for metabolite pools and pH during the early stationary phase, no significant differences were observed between the two glucose-loading conditions. ST was therefore carried out during the early stationary phase of cells under both the standard and limited glucose conditions.

Figure 2, f and f′, shows typical M^0 and M spectra obtained from *E. coli* cells at steady state under the standard conditions. The M^0 spectrum was obtained with the rf field positioned downfield from the P_i^{in}, as illustrated by the arrow. Apparent relaxation rates (T_1^{app}) were previously obtained from the inversion recovery experiments carried out during the steady-state saturation of the ATP peaks (data not shown). Using these parameters, the phosphate-to-ATP flux was calculated as described in Materials and Methods. The results indicate a 2.3-fold increase in the phosphate consumption rate under the standard glucose conditions as compared with that under the glucose-limited conditions (Table 2). It was shown that the increase in flux ($P_i \rightarrow$ ATP) correlates with the increase in glucose consumption between the two conditions (Tables 1 and 2). The rates of oxygen consumption increased 2.35-fold under the standard conditions, with no apparent changes in the ATP and ADP pool sizes between the two conditions observed. Therefore, ATP turnover coupled with oxidative phosphorylation must be drastically changed depending on glucose availability.

The energy-conversion competence of *E. coli* cells under the two glucose-loading conditions was estimated from the ATP turnover and the oxygen consumption rates. The apparent P/O ratios under the standard and limited glucose conditions were calculated as 1.4+/–0.3 and 1.5+/–0.1, respectively (Table 2). The rationality of these values will be discussed below based on the potential efficiency of respiratory enzymes.

Enzymatic activities of respiratory components- Two NADH dehydrogenases integrated into the *E. coli* respiratory chain are designated NDH-1 and NDH-2 (*2*). The H^+/e^- stoichiometry for *E. coli* NDH I is at least $1.5H^+/e^-$ (*26*). NDH-2 on the other hand, does not directly couple this reaction to any transmembrane charge movements (*i.e.*, $H^+/e^- = 0$) (*2*). The activities of the two NADH dehydrogenases were estimated and are summarized in Table 3. Under the standard glucose conditions, the two enzymatic activities decreased similarly with increases in cultivation times. NDH-1 activity during the ST period under standard and limited glucose conditions contributed 57% and 58% of the total NADH oxidizing activity, respectively (Table 3).

Two terminal oxidases of *E.coli* also differ in their H^+/e^- (*27*). The reported H^+/e^- values of the *bd*-type oxidase and *bo*-type oxidase are 1 and 2, respectively (*27*). There was greater *bo*-type oxidase activity than *bd*-type activity in the exponential phase, but this activity was drastically reduced as the cultivation process progressed (Table 3). The *bd*-type oxidase activity, on the other hand, was remained at constant levels throughout the cultivation period. The ratio of these two enzymatic activities shifted during the ST period (Table 3). The contributions of the *bo*-type activity to the total ubiqinol oxidizing activity under the standard and limited glucose conditions were approximately 32% and 36%, respectively (Table 3).

The H^+/ATP coupling ratio by F_0F_1-ATPase has been a matter of controversy for over three decades. However, van Walraven *et al.* provided clear evidence that the real H^+/ATP coupling ratio is 4 in chloroplasts and cyanobacteria (*28*), while Kashket determined the stoichiometry of the H^+-ATPase in *E. coli* under aerobic or anaerobic conditions to be 3 (*29*, *30*). This value was derived primarily from energy-balance measurements, and has been supported by others (*31*). Of these reported data, the transmembrane charge movement values in *E. coli* have suggested that the maximum P/O ratio is about 2.3 (H^+/ATP = 3), with the entire respiratory reaction occurring entirely between NDH-I and *bo*-type oxidase. The estimated P/O ratios in this study were very low compared with this theoretical maximum. Under our experimental conditions, the NDH-1 activity contributed primarily to the total NADH oxidizing activities in wild- type *E. coli*

Table 3. **Enzymatic activities of respiratory components in *E. coli* cells.**

Conditions (Phase)	NDH-1	NDH-2	bo-type	bd-type	NDH-1/Total (%)	bo-type/Total (%)
	(μmol/s/mg of protein)					
Standard glucose						
(exponential: 3 h)	1.58 ± 0.07	1.11 ± 0.06	1.38 ± 0.12	1.01 ± 0.10	58.8 ± 2.4	57.9 ± 4.5
(exponential: 5 h)	1.35 ± 0.03	0.86 ± 0.03	0.70 ± 0.05	1.07 ± 0.04	61.0 ±1.4	39.6 ± 2.6
(early stationary: 8 h)	1.17 ± 0.01	0.88 ± 0.01	0.46 ± 0.03	0.98 ± 0.02	57.1 ± 0.5	32.0 ± 1.9
Limited glucose						
(early stationary)	0.97 ± 0.05	0.70 ± 0.03	0.42 ± 0.04	0.75 ± 0.05	58.1 ± 2.29	36.0 ± 3.7

Enzymatic activities were measured as described in "MATERIALS AND METHODS." Values are the mean ± SD.

cells. However, the *bd*-type oxidase appears to predominate over the *bo*-type, and this predominance would support the present low P/O^{app} ratio value. If this is the case, enhancing the expression of the *bo*-type oxidase or disrupting the *bd*-type oxidase gene could be effective in increasing both the P/O ratio and cellular yields.

High-cell density cultures have generally been used to obtain quantitative data for *in vivo* NMR analysis. Mistumori *et al.* have observed the phosphate-to-ATP flux of non-growing *E. coli* cells by the saturation-transfer technique, and suggested the P/O ratio to be 3.0 (*15*). This P/O ratio is higher than ours, which may be due to glucose-mediated aerobic or anaerobic acidogenesis. In fact, they reported that the saturation-transfer results in their study were derived primarily from the step of substrate-level phosphorylation (GAPDH/PGK step) in *E. coli* cells (*15*). We strictly controlled the culture acetate accumulation by DOT and glucose feeding to prevent the effects of such substrate-level phosphorylation on the results, which might be the reason for the lower P/O ratio.

The P/O ratios have also been reported as 1.46 and 1.33 in both *E. coli* and *Bacillus subtilis,* respectively, based on stoichiometric estimations (*1*, *32*), and these values are comparable with our present data. Such a mathematical model, however, needs to be verified with the aid of biological data such as the biomass yield per ATP, as these biological parameters can be changeable depending on the culture conditions, while the biological parameters in the NMR method can be obtained directly from the dynamic metabolic situations. Thus, we believe that the mathematical model is more suitable for the describing static metabolic conditions, and the NMR method is suitable for real-time estimations of dynamic changes in various cultures.

In summary, the apparent P/O ratio obtained by our proposed system can represent the energetic competence through oxidative phosphorylation. The present methods, therefore, provides us with an extra tool for characterizing the aerobic respiratory system. In the future, we will construct mutants with different respiratory enzymatic activities, which will allow our *in vivo* NMR system to carry out more quantitative analyses.

REFERENCES

1. Neijssel, O.M. and Teixeira, de Mattos, M.J. (1994) The energetics of bacterial growth: a reassessment. *Mol. Microbiol.* **13**, 172–182
2. Calhoun, M.W., Oden, K.L., Gennis, R.B., de Mattos, M.J., and Neijssel, O.M. (1993) Energetic efficiency of *Escherichia coli*: effects of mutations in components of the aerobic respiratory chain. *J. Bacteriol.* **175**, 3020–3025
3. Bogachev, A.V., Murtazina, R.A., and Skulachev, V.P. (1993) Cytochrome d induction in *Escherichia coli* growing under unfavorable conditions. *FEBS Lett.* **336**, 75–78
4. Miller, M.J. and Gennis, R.B (1985) The cytochrome d complex is a coupling site in the aerobic respiratory chain of *Escherichia coli*. *J. Biol. Chem.* **260**, 14003–14008
5. Cotter, P.A., Chepuri, V., Gennis, R.B., and Gunsalus, R.P. (1990) Cytochrome o (cyoABCDE) and d (cydAB) oxidase gene expression in *Escherichia coli* is regulated by oxygen, pH, and the *fnr* gene product. *J. Bacteriol.* **172**, 6333–6338
6. Spiro, S., Roberts, R.E., and Guest, J.R. (1989) FNR-dependent repression of the *ndh* gene of *Escherichia coli* and metal ion requirement for FNR-regulated gene expression. *Mol. Microbiol.* **3**, 601–608
7. Jones, C.W., Brice, J.M., Downs, A.J., and Drozd, J.W. (1975) Bacterial respiration-linked proton translocation and its relationship to respiratory-chain composition. *Eur. J. Biochem.* **52**, 265–271
8. Gould, J.M. (1978) The kinetics of oxygen-induced proton efflux and membrane energization in *Escherichia coli*. *Prog. Clin. Biol. Res.* **22**, 567–578
9. Setty, O.H., Hendler, R.W., and Shrager, R.I. (1983) Simultaneous measurements of proton motive force, delta pH, membrane potential, and H^+/O ratios in intact *Escherichia coli*. *Biophys. J.* **43**, 371–381
10. Stouthamer, A.H., and Bettenhaussen, C.W. (1975) Determination of the efficiency of oxidative phosphorylation in continuous cultures of *Aerobacter aerogenes*. *Arch. Microbiol.* **102**, 187–192
11. Stouthamer, A.H. and Bettenhaussen, C.W. (1977) A continuous culture study of an ATPase-negative mutant of *Escherichia coli*. *Arch. Microbiol.* **113**, 185–189
12. Brown, T.R., Ugurbil, K., and Shulman, R.G. (1977) ^{31}P nuclear magnetic resonance measurements of ATPase kinetics in aerobic *Escherichia coli* cells. *Proc. Natl Acad. Sci. USA* **74**, 5551–5553
13. Campbell-Burk, S.L., Jones, K.A., and Shulman, R.G. (1987) ^{31}P NMR saturation-transfer measurements *in Saccharomyces cerevisiae*: characterization of phosphate exchange reactions by iodoacetate and antimycin A inhibition *Biochemistry* **26**, 7483–7492
14. Thoma, W.J. and Ugurbil, K. (1987) Saturation-transfer studies of ATP-P_i exchange in isolated perfused rat liver. *Biochim. Biophys. Acta* **893**, 225–231
15. Mitsumori, F., Rees, D., Brindle, K.M., Radda, G.K., and Campbell, I.D. (1988) ^{31}P-NMR saturation transfer studies of aerobic *Escherichia coli* cells. *Biochim. Biophys. Acta* **969**, 185–193
16. Alam, K.Y., and Clark, D.P. (1989) Anaerobic fermentation balance of *Escherichia coli* as observed by in vivo nuclear magnetic resonance spectroscopy. *J. Bacteriol.* **171**, 6213–6217
17. Luli, G.W., and Strohl, W.R. (1990) Comparison of growth, acetate production, and acetate inhibition of *Escherichia coli* strains in batch and fed-batch fermentations. *Appl. Environ. Microbiol.* **56**, 1004–1011
18. Noguchi, Y., Shimba, N., Toyosaki, H., Ebisawa, K., Kawahara, Y., Suzuki, E., and Sugimoto, S. (2002) In vivo NMR system for evaluating oxygen-dependent metabolic status in microbial culture. *J. Microbiol. Methods.* **51**, 73–82
19. Noguchi, Y., Shimba, N., Kawahara, Y., Suzuki, E., and Sugimoto, S. (2003) ^{31}P NMR studies of energy metabolism in xanthosine-5′-monophosphate overproducing *Corynebacterium ammoniagenes*. *Eur. J. Biochem.* **270**, 2622–2626
20. Kita, K., Konishi, K., and Anraku, Y. (1986) Purification and properties of two terminal oxidase complexes of *Escherichia coli* aerobic respiratory chain. *Methods Enzymol.* **126**, 94–113
21. Matsushita, K., Ohnishi, T., and Kaback, H.R. (1987) NADH-ubiquinone oxidoreductases of the *Escherichia coli* aerobic respiratory chain. *Biochemistry* **26**, 7732–7737
22. Shanks, J.V. (2001) In situ NMR systems. *Curr. Issues Mol. Biol.* **3**, 15–26
23. Slonczewski, J.L., Rosen, B.P., Alger, J.R., and Macnab, R.M. (1981) pH homeostasis in *Escherichia coli*: measurement by ^{31}P nuclear magnetic resonance of methylphosphonate and phosphate. *Proc. Natl. Acad. Sci. USA* **78**, 6271–6275
24. Alger, J.R., den Hollander, J.A., and Shulman, R.G. (1982) In vivo phosphorus-31 nuclear magnetic resonance saturation transfer studies of adenosinetriphosphatase kinetics in *Saccharomyces cerevisiae*. *Biochemistry* **21**, 2957–2963
25. Yang, Y.T., Bennett, G.N., and San, K.Y. (1999) Effect of inactivation of *nuo* and *ack*A-*pta* on redistribution of metabolic fluxes in *Escherichia coli*. *Bioechnol. Bioeng.* **65**, 291–297
26. Bogachev, A.V., Murtazina, R.A., and Skulachev, V.P. (1996) H^+/e^- stoichiometry for NADH dehydrogenase I and dimethyl

sulfoxide reductase in anaerobically grown *Escherichia coli* cells. *J. Bacteriol.* **178**, 6233–6337
27. Puustinen, A., Finel, M., Haltia, T., Gennis, R.B., and Wikstrom, M. (1991) Properties of the two terminal oxidases of *Escherichia coli*. *Biochemistry* **30**, 3936–3942
28. Van Walraven, H.S., Strotmann, H., Schwarz, O., and Rumberg, B. (1996) The H^+/ATP coupling ratio of the ATP synthase from thiol-modulated chloroplasts and two cyanobacterial strains is four. *FEBS Lett.* **379**, 309–313.
29. Kashket, E.R. (1982) Stoichiometry of the H^+-ATPase of growing and resting, aerobic *Escherichia coli*. *Biochemistry* **21**, 5534–5538
30. Kashket, E.R. (1983) Stoichiometry of the H^+-ATPase of Escherichia coli cells during anaerobic growth. *FEBS Lett.* **154**, 343–346
31. Fillingame, R.H. and Divall, S. (1999) Proton ATPases in bacteria: comparison to *Escherichia coli* F1Fo as the prototype. *Novartis Found Symp.* **221**, 218–229
32. Sauer, U. and Bailey, J.E. (1999) Estimation of P-to-O ratio *in Bacillus subtilis* and its influence on maximum riboflavin yield. *Biotechnol. Bioeng.* **64**, 750–754